Video Article

Wind Tunnel Experiments to Study Chaparral Crown Fires

Jeanette Cobian-Iñiguez[1], AmirHessam Aminfar[1], Joey Chong[2], Gloria Burke[2], Albertina Zuniga[1], David R. Weise[2], Marko Princevac[1]

[1]Department of Mechanical Engineering, University of California, Riverside

[2]Pacific Southwest Research Station, USDA Forest Service

Correspondence to: Jeanette Cobian-Iñiguez at jcobi002@ucr.edu

URL: https://www.jove.com/video/56591
DOI: doi:10.3791/56591

Keywords: Engineering, Issue 129, Chaparral, wind tunnel, surface fire, crown fire, fuel mass loss, flame height

Date Published: 11/14/2017

Citation: Cobian-Iñiguez, J., Aminfar, A., Chong, J., Burke, G., Zuniga, A., Weise, D.R., Princevac, M. Wind Tunnel Experiments to Study Chaparral Crown Fires. *J. Vis. Exp.* (129), e56591, doi:10.3791/56591 (2017).

Abstract

The present protocol presents a laboratory technique designed to study chaparral crown fire ignition and spread. Experiments were conducted in a low velocity fire wind tunnel where two distinct layers of fuel were constructed to represent surface and crown fuels in chaparral. Chamise, a common chaparral shrub, comprised the live crown layer. The dead fuel surface layer was constructed with excelsior (shredded wood). We developed a methodology to measure mass loss, temperature, and flame height for both fuel layers. Thermocouples placed in each layer estimated temperature. A video camera captured the visible flame. Post-processing of digital imagery yielded flame characteristics including height and flame tilt. A custom crown mass loss instrument developed in-house measured the evolution of the mass of the crown layer during the burn. Mass loss and temperature trends obtained using the technique matched theory and other empirical studies. In this study, we present detailed experimental procedures and information about the instrumentation used. The representative results for the fuel mass loss rate and temperature filed within the fuel bed are also included and discussed.

Video Link

The video component of this article can be found at https://www.jove.com/video/56591/

Introduction

In 2016, the state of California experienced a total of 6,986 wildland fires, consuming 564,835 acres[1], costing millions of dollars in damage, and risking the wellness of hundreds of people. Because of the regional Mediterranean climate, a major fuel source for these fires are chaparral vegetation communities[2]. Fire spread in chaparral can be considered a crown fire since the main fuel that burns is elevated[3]. Co-existing with the predominantly live crown layer, is the dead surface fuel layer, which consists of cast foliage, branches, and herbaceous plants which grow under and between the individual shrubs. Fire will more easily initiate in the dead surface fuel layer. Once the surface fire ignites, the fire may transition to the crown layer where the energy released by the fire increases dramatically. While chaparral fires have typically been modelled as a fire spreading in deep surface fuels[4], there has been limited study of chaparral fires as crown fires.

Crown characteristics in chaparral, including foliage particle shape, differ from boreal coniferous forest, where most of the research has occurred. Numerous laboratory and field scale studies have investigated various aspects of wildfire dynamics[6,5,7,3,8,9,10,11,12]. Within the realm of laboratory experiments, several studies have examined the influence of parameters such as wind and fuel properties on chaparral crown fire behavior. Lozano[7] examined characteristics of crown fire initiation in the presence of two discrete crown fuel beds. In Tachajapong *et al.*[3], discrete surface and crown layers were burned inside a wind tunnel and the surface fire was characterized. Only crown fire initiation was fully described leaving full analysis of spread for future work. Li *et al.*[11] reported on the propagation of a flame though single chaparral shrubs. In related work, Cruz *et al.*[10,9] developed a model to predict the ignition of coniferous foliage above a spreading surface fire. Burn characteristics of chaparral fuels have been explored in experimental studies of bulk fuels and individual leaves[13,14,15,16]. Dupuy *et al.*[13] studied the burning characteristics of *Pinus pinaster* needles and excelsior by burning the fuels in cylindrical baskets. They observed that in these fuels, flame height was related to heat release rate via a two-fifths power law as has been reported previously in the literature[17,18]. Sun *et al.*[14] burned chaparral fuels in similar cylindrical baskets to analyze the burning characteristics of three chaparral fuels: chamise (*Adenostoma fasciculatum*), ceanothus (*Ceanothus crassifolius*), and manzanita (*Arctostaphylos glandulosa*).

Motivated by results from the aforementioned laboratory studies, our purpose here is to present a methodology to characterize spread in both surface and shrub crown layers. Furthermore, we aim to clarify some of the key characteristics that dictate the degree of surface-crown layer interaction. To this purpose, we developed an experimental laboratory methodology to study the vertical transition of a fire burning in a wildland surface fuel to a fire spreading in an elevated shrub fuel. In these types of fires, translation of the fire to the shrub crown, known as crowning, may be followed by sustained spread under the right conditions. In general, chaparral fire behavior is dictated by topography, weather, and fuel[19]. It has been shown that wind affects energy release rate in the fuels[5,3,8,20].

Fire spread in porous fuels can be viewed as a series of transitions or thresholds that must be crossed to be successful[21]. Energetically, a fuel particle ignites if the amount of heat that it receives results in a mixture of gases that successfully react with oxygen. The resulting flame spreads

if the heat from the burning particle ignites an adjacent fuel particle. The fire spreads across the ground if it is able to cross gaps between combustible fuel elements. If the flame of a surface fire is able to propagate vertically into the crown of shrubs and trees, a significant change in fire behavior, including increased heat release rates, is often observed due to a greater availability of fuel. Thermal energy dynamics in wildland fires encompass several scales, from the very large scale, such in mega-fires which often require climatological modeling, to the small scale requiring chemical scale kinetic modeling. Here, we deal with laboratory wind tunnel scale behavior modeling; for chemical scale cellulose combustion studies, the reader is referred to works such as Sullivan *et al.*[22]

Since 2001, we have conducted a variety of experiments examining some of the laboratory scale energy thresholds[23,8,24,25,26,27], with an emphasis on live fuels associated with chaparral. While outdoors measurements of fire may provide more lifelike results, the controlled environment of the wind tunnel allow for delineation of the impact of various parameters. Controlling wind, for example, is especially important for chaparral crown fires occurring in regions such as Southern California where foehn type winds, known as Santa Ana winds, are typical drivers of fire events. Because a major motivator for the methodology described here is to study the effect of wind and other controlled parameters on chaparral fire spread, this study was performed in a laboratory scale wind tunnel. The reader is directed to the work by Silvani *et al.*[28] for field measurements of temperature in chaparral fires similar to the ones presented here. For field measurements on the effect of wind on fire spread, please see Morandi *et al.*[29]

Several parameters influencing the spread in chaparral fuels have been experimentally analyzed by quantifying the probability of fire spread success in elevated fuel beds[8]. The current experimental study involves a methodology developed to study chaparral crown fire spread by modeling surface fuels and crown fuels inside the test section of a low speed wind tunnel. The surface fuel is modeled with excelsior (dried shredded wood). The surface fuel bed is placed on the ground level of the wind tunnel over a standard scale (see **Figure 1**). Representing the crown fuel bed, a fuel bed with chamise was placed over the surface fuel bed by suspending the fuel from a platform mounted on the wind tunnel frame (see **Figure 1**). Both fuel beds are instrumented for temperature and mass loss measurements; flame geometry is obtained from video recordings of experiments. Parameters measured include mass loss rate, fuel moisture content and the relative humidity of the air. Parameters controlled were wind presence, distance between surface fuel bed and crown fuel bed, and the presence of surface fuel. The measured mass loss rate can be used to calculate the heat release rate, which is defined as:

$$Q = -h\frac{dm}{dt} \qquad (1)$$

where h is the heat of fuel combustion, m is the fuel mass, and t is time.

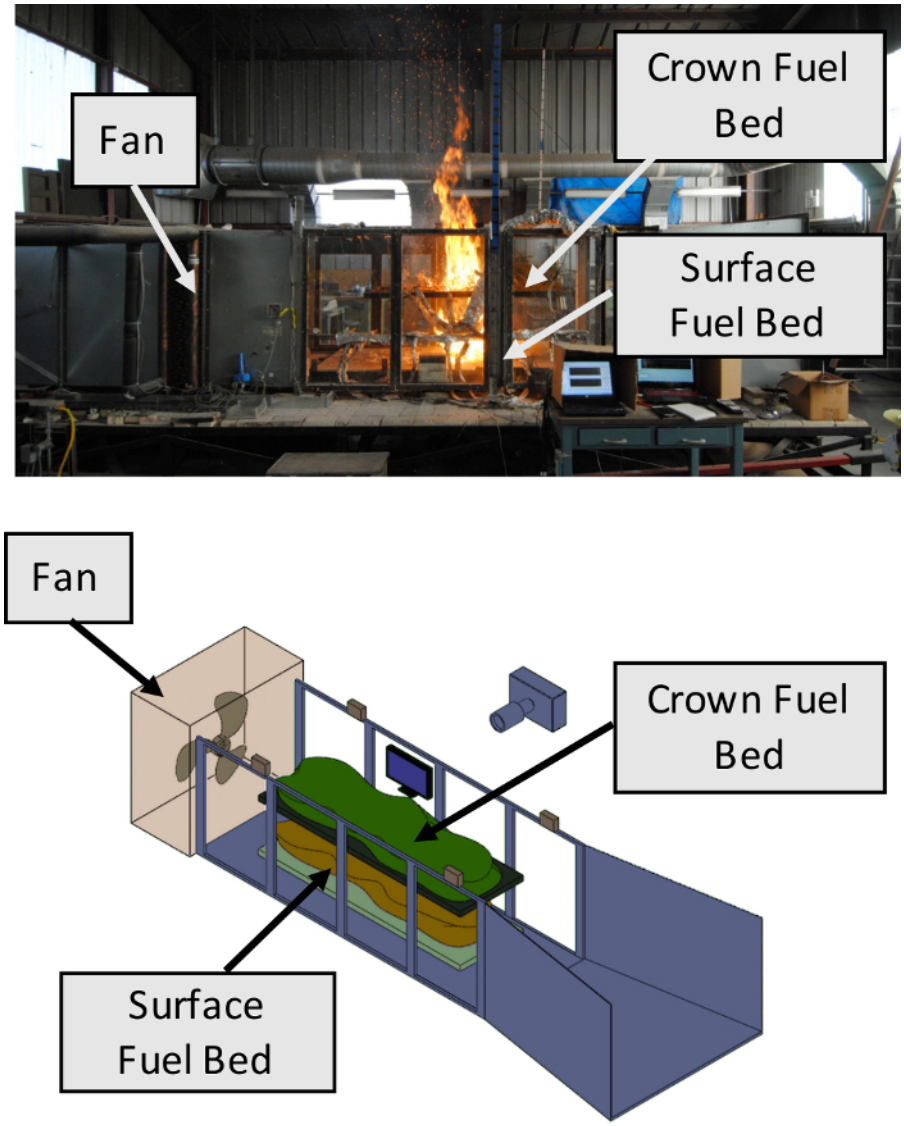

Figure 1: Wind tunnel experimental setup. Locations of the crown fuel bed, the surface fuel bed, and the tunnel fan have been labeled for convenience. The surface fuel bed is placed on the ground level of the wind tunnel over a standard scale. Representing the crown fuel bed, a fuel bed with chamise was placed over the surface fuel bed by suspending the fuel from a platform mounted on the wind tunnel frame. Please click here to view a larger version of this figure.

Experiments have focused on understanding the behavior of chaparral crown fires, particularly ignition, mechanisms of flame propagation and spread, flame front velocities, and fuel consumption rates.To study the interaction between a surface fire and a crown fire, six configurations of surface and crown fuel beds with and without applied wind flow, have been burned in the wind tunnel: crown fuel only with and without wind (2), crown and surface fuel beds separated by two distances with and without wind (4). **Table 1** summarizes the experimental configurations with the 6 experimental classes. In the table, the surface fuel bed parameter denotes whether surface fuel was present during the experiment, the wind parameter refers to the presence of wind and crown height refers to the distance between the bottom of the crown fuel bed and the bottom of the surface fuel bed. Fuel moisture was measured for each experiment but not controlled, average fuel moisture content was 48%, whereas the minimum and maximum values were 18% to 68%, respectively.

Class	Surface Fuel Bed	Wind	Crown Height
A	Absent	No wind	60 or 70 cm
B	Absent	1 ms^{-1}	60 or 70 cm
C	Present	No wind	60 cm
D	Present	No wind	70 cm
E	Present	1 ms^{-1}	60 cm
F	Present	1 ms^{-1}	70 cm

Table 1: Experiment configurations. Here the surface fuel bed parameter denotes whether surface fuel was present during the experiment, the wind parameter refers to the presence of wind and crown height refers to the distance between the bottom of the crown fuel bed and the bottom of the surface fuel bed.

An electronic scale measured surface fuel mass and we developed a custom mass loss system for the crown layer. The system consisted of individual load cells connected to each corner of the suspended fuel bed. Consumer-grade video cameras recorded the visual flames; image processing of the visual data using a custom script generated flame characteristics including height and angle. A program was developed to convert video frames from RGB (red/green/blue) coding to black and white through a process of light intensity thresholding. The edge of the flame was obtained from the black and white video frames. Maximum flame height was defined as the highest point of the flame edge, instantaneous flame heights were also obtained. In an image, flame height was measured from the base of the fuel bed to the maximum vertical point of the flame. All processing codes as well as the instrument control interface designed for this protocol have been made available by the authors here through their software access site. Harvesting the live fuel locally and conducting the experimental burns within 24 h minimized moisture loss. A thermocouple array recorded fuel bed temperature in the wind stream-wise direction enabling the calculation of spread rate. **Figure 1** shows a diagram of the fuel bed setup along with the thermocouple arrangement. Details of the experimental protocol follow.

Protocol

Caution: As several steps in the following protocol involve activities that have the potential to cause injury, ensure that the proper personal protective equipment (PPE) is used following established safety protocols including fire resistant clothing and protective eyewear.

1. Crown Fuel Bed Load Cell Instrumentation Setup

1. Modify 4 C-clamps by attaching dual spring gate carabiners (see **Table of Materials**) through the pin hole at the clamp's screw end (see **Figure 2**). Use the carabiners to suspend the crown fuel bed.
2. Using a different set of C-clamps, affix each load strain gauge cell to the top portion of the wind tunnel frame (see **Figure 2**).
3. Attach modified C-clamps to the free end of the strain gauge cells, with the carabiners hanging down. Attach chains to the platform for the crown fuel bed.
4. To suspend the crown fuel bed platform from the wind tunnel frame, connect each of the crown fuel bed chains to a carabiner.
5. Once each of the four load cells are fully mounted and connected to the fuel bed, connect their wires to the Wheatstone bridge which will be used for data acquisition. Cover the load cells with fire insulating material, such as the kind used for fire shelters.

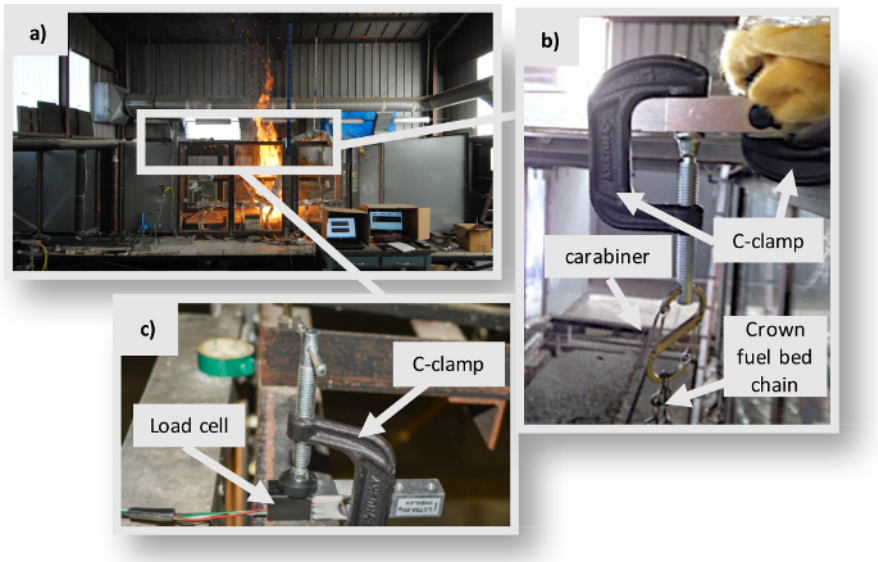

Figure 2: Wind tunnel crown fuel bed load cell instrumentation. (**a**) Wind tunnel front view (**b**) Modified C-clamp with carabiner and crown fuel bed chain which supports the crown fuel bed. (**c**) Load cell attached to the wind tunnel frame using a C-clamp. Please click here to view a larger version of this figure.

2. Load Cell Calibration

NOTE: The signal produced by the load cells is converted to an equivalent mass through:

$$m = A \cdot V + B \quad (2)$$

where *V* is the signal, typically in millivolts, *A* and *B* are constants to be determined through calibration, and *m* represents the mass in grams. All the parameters in equation (2) are obtained through the custom instrument control interface developed for the crown mass instrumentation in this protocol. When first using the system, precision weights are used to calibrate the load cell signal. Calibration constants *A* and *B* will be obtained based on the signal produced when measuring the load of these precision weights. The constant *A* is calculated from:

$$A = \frac{m_t}{a_w - a_{w,o}} \quad (3)$$

where m_t is a the mass of trial precision weight, a_w is the signal produced with the weight loaded on the load cell, whereas $a_{w,o}$ corresponds to the signal produced when no weight is applied on the load cell.

1. To obtain the calibration constant *A*, hook precision weights (a good range would be 200 - 500 g) to the first load cell. Use the mass of the precision weights as parameter m_t in equation (3).
2. Set the load cell gain to 128 using the Input # field as shown in **Figure 3b**, i.1. This corresponds to the maximum value allowed by the device.
3. Read the signal output at Output 0 from the instrument interface (See **Figure 3b**, i2). This is parameter a_w in equation (3).
4. Unhook the weight and read the new value displayed in the instrument interface (**Figure 3b**, i2). This is parameter $a_{w,o}$.
5. Calculate *A* based on the parameters (m_t, a_w, $a_{w,o}$) obtained in steps 2.1 to 2.4 and the equations presented.
6. In the controller interface, fill in the Ch 0-M value for each sensor with the *A* value obtained in the previous step.
7. To find the offset value, *B*, remove all weights, read the value in the 'Outputs Calibrated (g)' box (See **Figure 3c, i2**), multiply this value by -1. The resulting number is constant B, type this number in the "Addition" Ch 0-A box (See **Figure 3c**, i.3).
8. Repeat steps 2.3 - 2.8 for each load cell (0, 1, 2, 3), the system is now completely calibrated; proceed to load the fuel beds with the fuels.

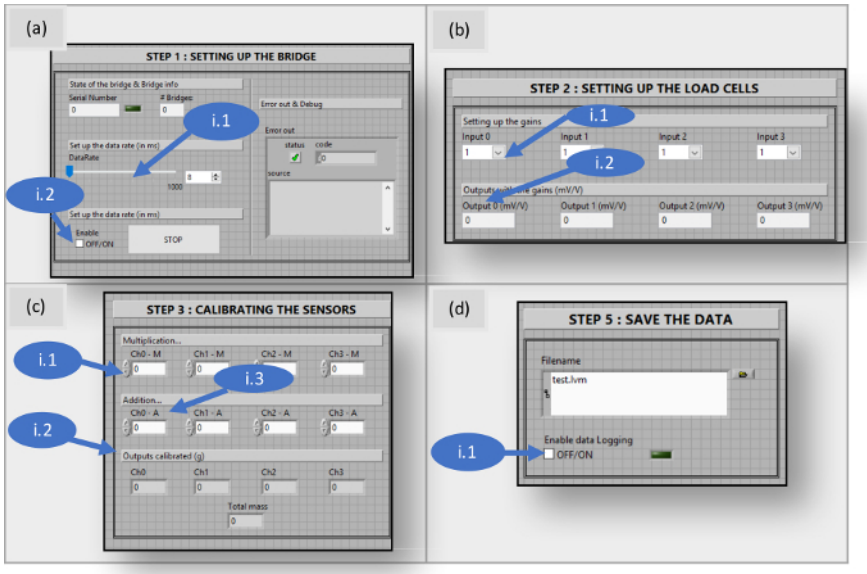

Figure 3: Instrument control interface data input steps for load cell calibration. (**a**) Bridge initial setup window with gain setup and enable box (**b**) Window for first stage of load cell calibration (**c**) Window for second stage of load cell calibration (**d**) Window for last stage of load cell calibration, file is saved here and data logging was started. Please click here to view a larger version of this figure.

3. Preparation of Chaparral and Excelsior Fuel Beds

NOTE: Each experiment uses 2 kg of live chamise and 0.5 kg of excelsior (shredded aspen wood).

1. From the pile of fuel collected for burning, collect several 1-pint bottles of fuel (3 - 4 bottles).
    1. Follow the procedures delineated by Countryman and Dean to oven dry samples and obtain fuel moisture content[30].
2. Trim individual branches from a bundle of recently harvested chamise to remove dead material and branch material greater than ¼ inch diameter. Place the remaining live fuel material in the container for weighing.
3. Select 2 kg of the trimmed chamise and 0.5 kg of excelsior using an electronic scale. Place 0.5 kg of excelsior onto the surface fuel bed platform on the wind tunnel floor, ensuring that the bulk density is as uniform as possible. Do this by placing a known amount of excelsior over a known area depth.
4. Pull apart (fluff) the compacted excelsior to decrease its bulk density so it will burn readily. Load 2 kg of trimmed chamise onto the platform hanging from the load cells to create the elevated fuel bed. Evenly spread the chamise branches over the entire platform to produce a uniform fuel bed.

4. Thermocouple Arrangement

NOTE: K-Type thermocouples are used to measure temperature of both fuel beds. Data is collected through a data acquisition system controlled with a custom graphical user interface (see table of materials for controller design software). The thermocouples recommended for use are 24 AWG thermocouples with a response time of 0.9 s.

1. Connect an array of sixteen 24 AWG thermocouples (conductor diameter: 0.51054 mm) to a data logger (response time: 0.9 s).
2. Insert 6 thermocouples into the crown fuel layer. Place these thermocouples 20 cm apart and avoid contact of thermocouples with branches. Insert 10 thermocouples into the surface fuel layer. Place these surface fuel thermocouples 10 cm apart and avoid contact of thermocouples with branches (See **Figure 4**).
3. Activate data logging by clicking the "Start" button in the thermocouple control software interface.

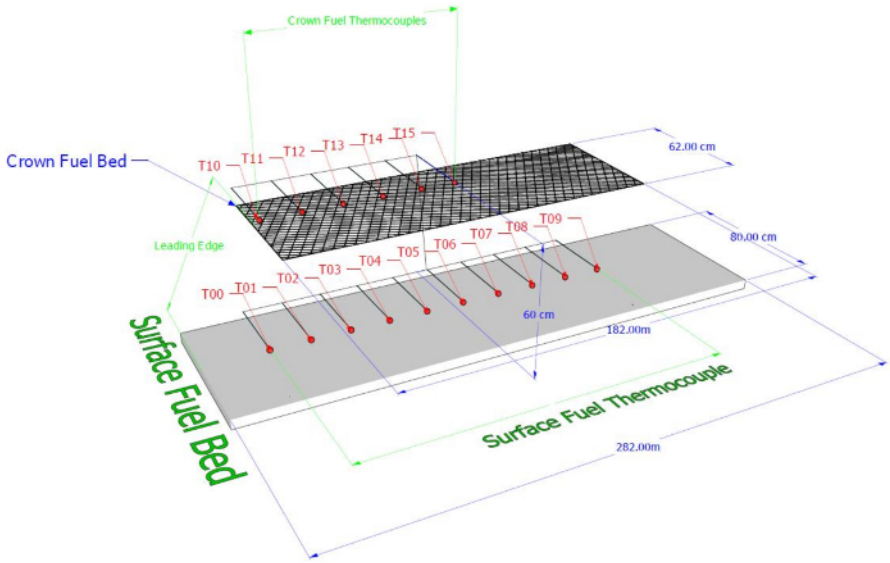

Figure 4: Diagram of surface and crown fuel beds with thermocouple array location. Here 6 thermocouples were inserted into the crown fuel layer 20 cm apart from each other. 10 thermocouples were inserted into the surface fuel layer 10 cm apart. Please click here to view a larger version of this figure.

5. Image Acquisition Setup

1. Mount the visual reference target that has red marks at 10-cm-intervals above the wind tunnel window. Use this target as a reference to determine flame height from the experiment video.
   NOTE: Sample flame heights are presented in **Figure 5**.
2. Setup photographic data collection. Focusing on the wind tunnel test area, adjust the camera focus so as to capture the entire vertical reference target as well as the fuel bed area.
3. Setup video camera data collection. Mount the video camera with a universal camera wall mount on the wall to provide a full view of the wind tunnel test section.

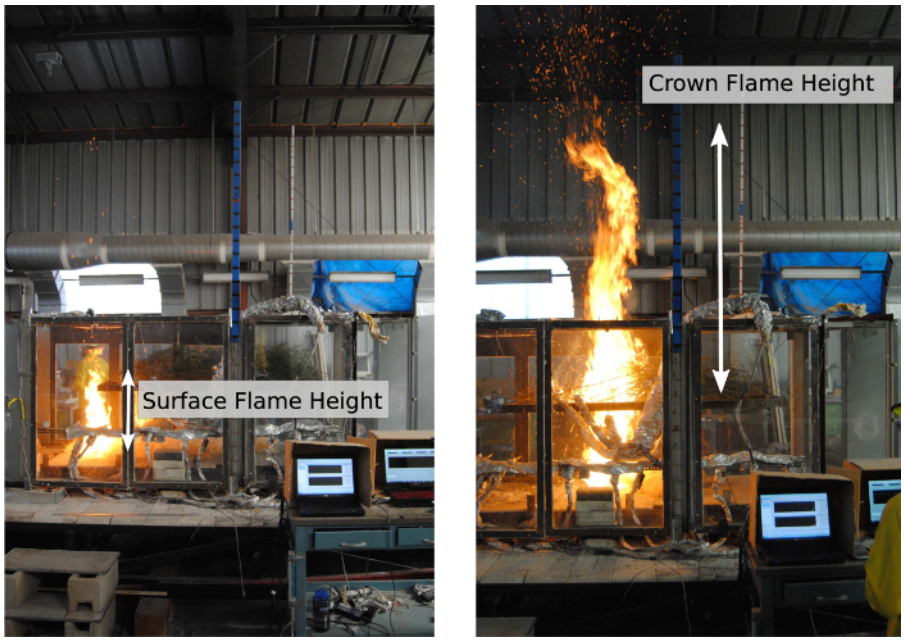

Figure 5: Photograph of sample flame heights from a typical experiment. The blue visual target with red marking serves as a reference to determine flame height from the experiment video. Please click here to view a larger version of this figure.

6. Flow Setup

NOTE: The wind tunnel is equipped with a variable speed fan. The air flow in the wind tunnel has been previously calibrated to the fan speed. To achieve the desired wind velocity, the fan rotational speed (in Hz) is selected. In the present experiments, no wind and 1 m/s wind flow cases were studied.

1. Set the fan speed to 1 m/s on the speed controller. Turn on the fan to ensure that it is functioning properly.
2. Turn off the fan. It is now ready for use.
   NOTE: The burn building is designed to conduct fire experiments safely while evacuating smoke from the working space. Notify local fire authorities that experiments are being conducted to eliminate the occurrence of false alarms.
3. Close all doors in the building to ensure that the roof vents are the only possible exit for smoke evacuation.
4. Turn on the air supply fans to bring in fresh air from outside the building at floor level. Turn on the exhaust fans to evacuate smoke through the roof vents.
   NOTE: This will establish a low velocity, high volume air flow from outside the building that rises vertically due to the slight pressure difference and the roof openings.
5. Prior to each experiment, use a wet-bulb hygrometer to measure the relative humidity and temperature of the ambient air.

7. Ignition (Implement Simultaneously with Step 8)

NOTE: The ignition process should be conducted as follows by the ignition crew member. For increased safety, it is recommended that a second crew member remain near the test area during ignition.

1. When instructed to 'ignite', soak the leading edge of the excelsior surface fuel bed with denatured ethyl alcohol. Place the alcohol bottle away from the ignition zone and using a butane torch, ignite the end of the surface fuel bed in a line parallel to leading edge of the fuel bed. Be observant as the alcohol-soaked fuel will readily ignite.
2. Once the fuel bed has been ignited, step out of the test section and close the tunnel door. If wind is required for the experiment, turn on the wind tunnel fan.

8. Initiate Experimental Run

NOTE: Upon verifying the experiment is correctly setup, the cameras should be started.

1. Turn on the video camera to record.
2. Speak aloud the experiment number/code, the date, and experimental configuration so the microphone on the video camera records this information.
3. Instruct the computer crew to begin data logging by ticking the "Enable data logging" option in the instrument control interface (see **Figure 3d**, i.1). Instruct the ignition person to ignite the fuel. Once the ignition crew member exits the wind tunnel, instruct the wind crew member to start the wind tunnel fan. This will be the start of the experiment where time is zero (t = 0).

Representative Results

Crown and surface flame height data were obtained from the video data. Typical flame height trends for experiments is presented in **Figure 6**. Flame height behavior followed that found in Sun *et al.*[14]

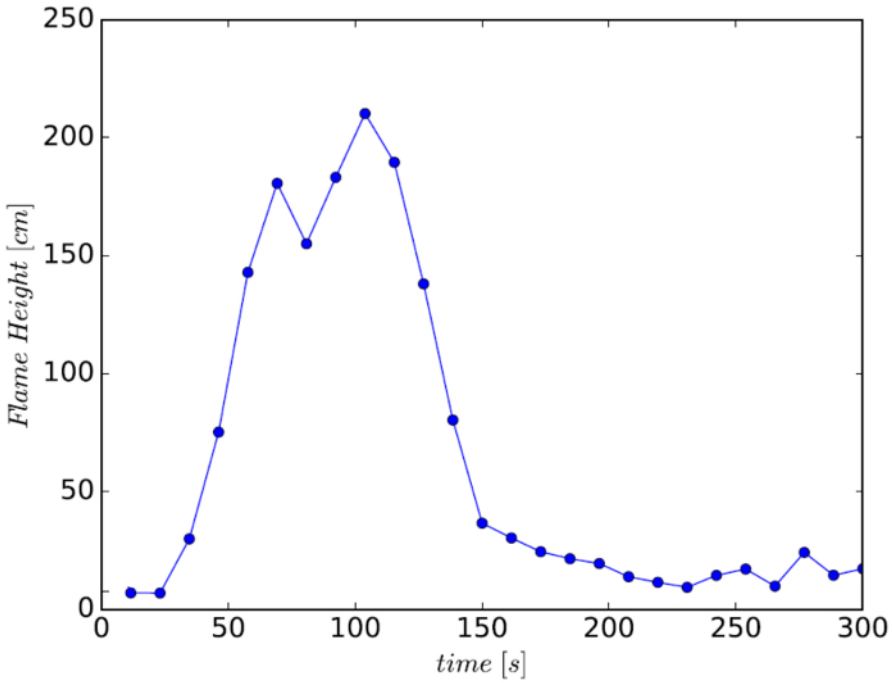

Figure 6: Estimated crown flame height. Here U = 1 m/s, surface-crown separation d = 70 cm. This corresponds to a representative Class E experiment. Flame height is obtained by processing images from the experiment video. Please click here to view a larger version of this figure.

The evolution of flame height in **Figure 6** was chosen because it shows typical flame height behavior for experiments with wind. In these types of experiments, the flames start small, get large close to the middle of the fuel bed, then will decay with time as flames get closer to the end of the fuel bed. The experiment in the presented figure is Case F (wind at 1m/s and distance between crown and surface fuel at 70 cm). In this case, the wind helps the flame to tilt. Because of the flame tilt, radiative heat transfer of the flame to the fuel bed is enhanced[31]. As the flame travels through the fuel bed it will pre-heat the fuel ahead of it. The mid fuel bed seems to be an optimum location where sufficient preheating has occurred over a large amount of fuel to create a large flame. The end of the fuel bed is also pre-heated, however, the amount of fuel becomes limited so that less pyrolysis gases are released which results in decreased flame height.

Fuel consumption rates were obtained for the entire extent of both fuel beds. The evolution of mass loss for selected experiments is presented in **Figure 7**. The non-dimensional parameter M is the ratio of instantaneous mass m and the initial mass m_0. Dimensionless time T is the ratio of the experimental time t and the total burn time t_f, where total burn time is defined as the time when flaming ignition has stopped. The evolution of mass loss throughout experiments followed expected behavior. Three general regions were identified from the characteristics of the mass loss curve: ignition, flaming, and smoldering, see **Figure 7**. This was a Case F experiment (wind at 1 m/s, distance between surface and crown of 70 cm). The fuel moisture content was 45%, relative humidity was 66%, and the total burn time was 2.5 min. Overall mass loss and mass loss rate trends matched those presented by Rothermel[32] and Freeborn *et al.*[33]

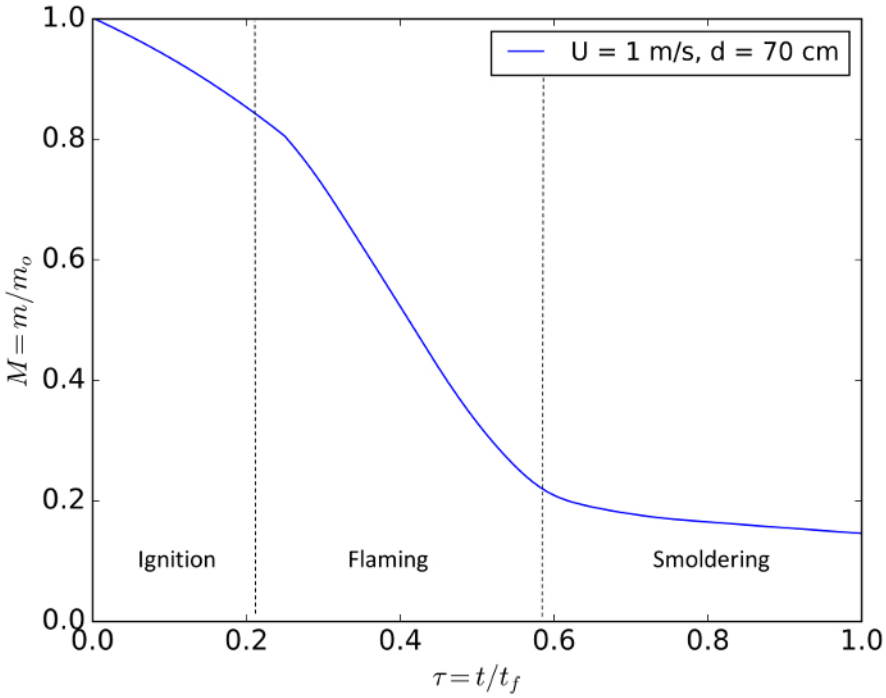

Figure 7: Fuel consumption trend. Depicted is a representative Class F experiment, where U = 1 m/s and surface-crown separation d = 70 cm. Combustion regions are labeled in the plot (ignition, flaming and smoldering). The generalized trend with these three regions was observed for most experiments. Please click here to view a larger version of this figure.

To illustrate mass loss trends for both the surface and crown layers obtained from experiments described through this methodology, the results for four experiments are presented in **Figure 8** and **Figure 9**. Average burn times for experimental categories represented by **Figure 8** were as follows: Class C and D averaged 4.5 minutes and class E and F averaged 2.5 minutes. As can be observed, wind enhanced the rate of mass loss and the total burn time.

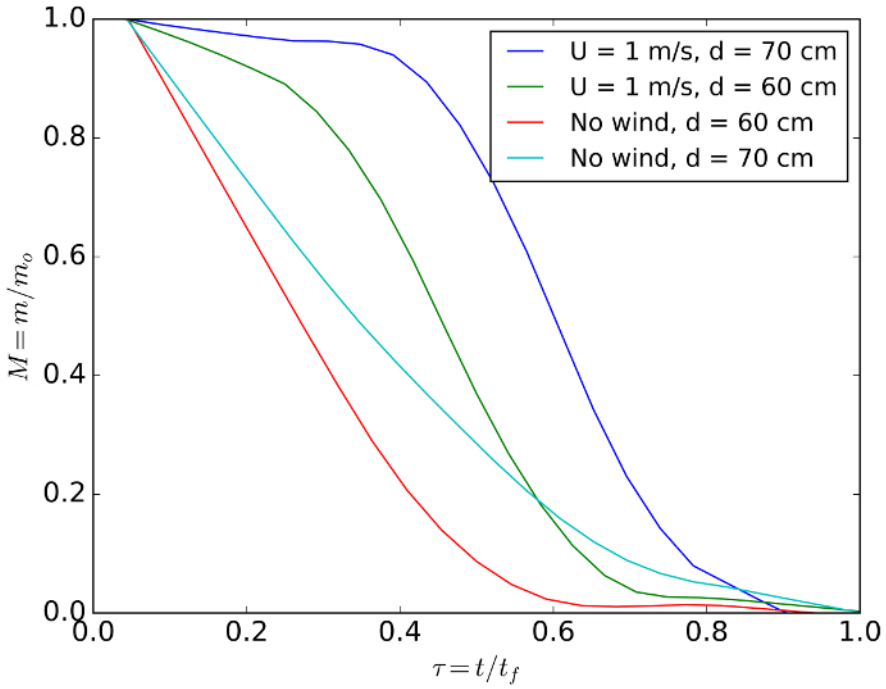

Figure 8: Surface fuel bed mass loss for representative experiments. Data are shown from experiments with wind at 1 m/s and without wind, as well as the two surface-crown distances tested: d = 60, 70 cm. Mass loss data here are obtained from the digital scale used for the surface fuel bed. Please click here to view a larger version of this figure.

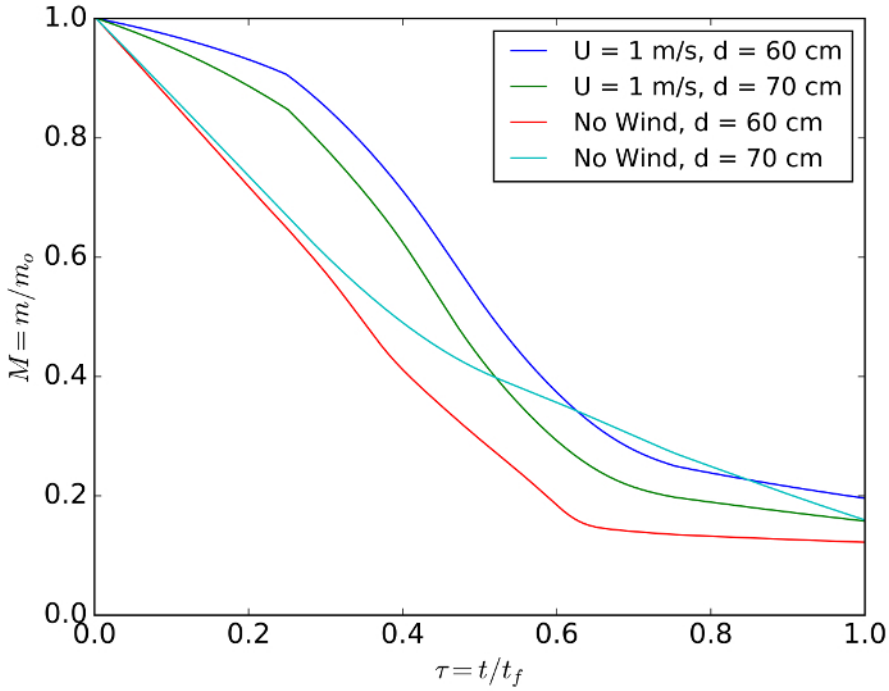

Figure 9: Crown fuel bed mass loss for representative experiments. Data show experiments with wind and without wind as well as the two surface-crown distances tested. Mass loss data here is obtained from the load cell instrumentation used for the crown fuel bed. Please click here to view a larger version of this figure.

Gas phase temperatures were measured for both fuel beds using sixteen thermocouples within the fuel beds. Thermocouples are labeled T0-T15, **Figure 4** depicts the thermocouple arrangement. Thermocouples T0-T09 were placed inside the surface fuel bed, while T10 - T15 were placed inside the crown fuel bed. Crown fuel bed temperatures for a selected experiment are presented in **Figure 10**.

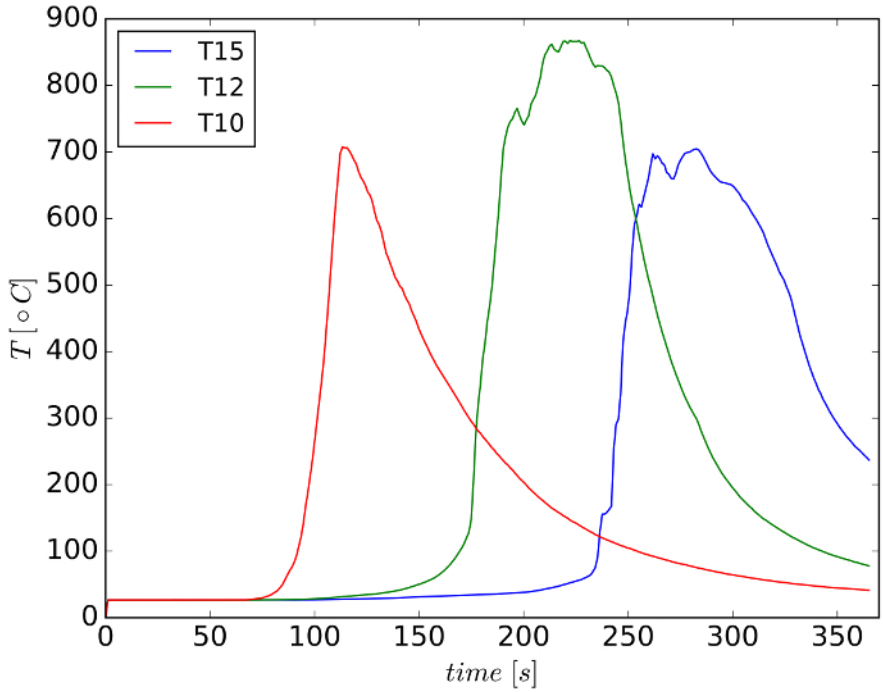

Figure 10: Fuel bed gas temperatures crown fuel bed. Thermocouple arrangement is indicated in **Figure 4**. Shown is a Class B experiment without surface fuel bed and a wind speed of 1 m/s. Please click here to view a larger version of this figure.

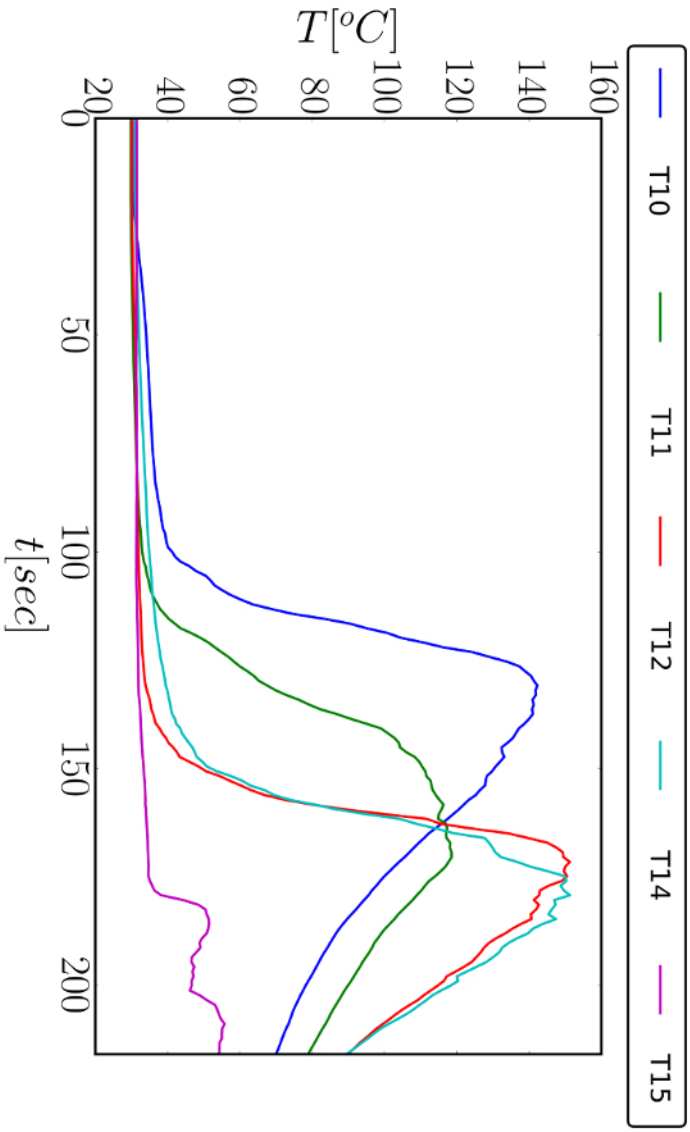

Figure 11: Temperature readings resulting from improper placing of thermocouples. Thermocouple arrangement is indicated in **Figure 4**. Depicted are data for crown fuel bed temperature where the thermocouples were improperly placed as is apparent by the abnormally low temperatures. Please click here to view a larger version of this figure.

It is important to note that if the thermocouples are not properly inserted in the fuel bed, temperature readings will be inaccurate. For instance, upon examining temperature readings in the experiment represented by **Figure 11**, it was noted that temperatures for one of the crown fuel bed thermocouples (T15) was below normal for burning conditions. These temperatures were closer to ambient conditions than to the gas phase temperatures of burning chamise. Thus, it was inferred that in this case, thermocouple T15 remained outside the fuel bed through the experiment.

Discussion

The ability to measure the elevated fuel mass throughout the experiment was one of the main advantages of the technique presented here. Previous studies addressing chaparral fire have focused on either only crown fire initiation or only on surface spread, but not both. Such studies have quantified the possibility of ignition in the crown layer and have left study of spread for future work[23]. Our methodology allows for measurement of mass loss, temperature distribution, and flame geometry for both layers involved in shrub crown fire ignition and spread. It provides a means for indirectly inferring energy flux from the rate of mass loss. Other studies have shown the advantages of directly measuring heat flux in fire spread experiments. Finney *et al.* presented several examples of heat flux measurements in wildfire spread experiments[34]. Through such work, they were able to make important observations on the roles convective and radiative heat transfer play in wildfire spread. The methodology presented here allowed for baseline observations of energy dynamics in wildfire spread in the chaparral. A beneficial next step would involve a more in-depth analysis of the particular contributions of radiative and convective heat transfer. For future studies, we recommend exploring the direct measurement of heat fluxes.

To ensure accuracy in the measurements there are several critical steps. The calibration of the load cells measuring crown mass loss is perhaps the most critical step and the step that takes the most time. This is because at the end of each experiment day, the crown fuel bed must be unmounted, and slight movement in the configuration may cause alterations in the mass readings. Hence, calibration must be done at the beginning of each experiment day. For future experiments, a more permanent configuration would be ideal. In this future configuration, the individual load cells would be affixed to the experimental setup.

In addition to the calibration step, another critical step in the protocol is the preparation of the fuels. The intent of the entire experimental program is to develop a better understanding of combustion in live fuels for the purpose of improving our ability to predict prescribed fire behavior. While live branches up to ½ inch (1.27 cm) can be consumed in the flame front of a high intensity prescribed burn in chaparral (see Green[35]), larger diameter fuels are typically not burned in the flame front. Laboratory burns using chaparral fuels have focused on using fuels that would generally be consumed by a prescribed burn's spreading flame front (see Cohen and Bradshaw[36], Weise *et al.*[37]). Major chaparral species include chamise (Adenostoma fasciculatum), while other chaparral fuels include manzanita (Arctostaphylos glandulosa) and hoaryleaf ceanothus (Ceanothus crassifolius). Here chamise was the fuel chosen because it is the most flammable of these species. The protocol can be modified to include other species as long as the branch size is maintained below ¼ inch.

In general, regardless of the species chosen as fuel, branches should be trimmed such that all branch diameters are < ¼ inch (0.63 cm) in order to maintain uniformity. Not performing this step or performing it incorrectly would negatively affect the reproducibility of the results. Over trimming the branches may also be disadvantageous because fuel beds with very small branch sizes tend to have greater packing density and hence also burn differently. In the procedure described here, following Omodan[38], the packing density was maintained at an average of 9.2 kg/m^3.

It is worth noting that because of the scale of this experiment, a crew of 4 or more people is required to ensure efficiency during the experiment. Having a person in charge of the crew with the protocol visible at all times is important to ensure all steps are followed correctly. This person is in charge of the safety of the crew as well as the coordination of the experiment. It is important that this person and the rest of the crew pay attention to their safety and that of the environment, which means having visibility of fire extinguisher, ensuring exhaust vents are on and the doors are closed during the experiment.

Additionally, it would be advantageous to synchronize all the instruments with a single trigger button. This would make data analysis and processing more efficient. Finally, a natural progression after the technique here is mastered would be to integrate some of the remaining wind tunnel capabilities such as temperature control which has been shown in other studies to be another important factor to consider. This would enable a wider range of control of environmental conditions. The results presented here are from experiments conducted during the summer months when fuels are typically drier; this period also corresponds to a portion of the year when wildland fires occur. If, however, a large range of seasons are to be analyzed during one experimental period, the wind tunnel temperature control may be employed. Similarly, variation of fuel moisture content would provide insight on the influence of this parameter on chaparral crown fire transition and spread. In designing an expanded study to include fuel moisture content and bulk density as controlled parameters, error analysis such as the one provided by Mulvaney *et al.* would aide in designing a methodology with experimental uniformity[39].

The technique described here enables an examination of crown fire behavior that integrates measurements of mass, temperature, and flame geometry for both layers of fuel involved. Analysis resulting from this methodology may lead to an increased understanding of chaparral fire as a crown fire specially within the bounds of independent, passive or active crown fire behavior as presented by Van Wagner[5], thus providing knowledge to aid in fire prediction and control.

Disclosures

The authors have nothing to disclose.

Acknowledgements

The authors would like to acknowledge Benjamin Sommerkorn, Gabriel Dupont, Jake Eggan and Chirawat Sanpakit who assisted with the experiments presented here. Jeanette Cobian Iñiguez acknowledges support by NASA MUREP Institutional Research Opportunity (MIRO) grant number NNX15AP99A. This work was also funded by the USDA/USDI National Fire Plan through an agreement between USDA Forest Service, PSW Research Station and the University of California - Riverside.

References

1. California Department of Forestry and Fire Protection. *Incident Information, 2016.* at <http://cdfdata.fire.ca.gov/incidents/> (2016).
2. Minnich, R. A. Fire mosaics in southern California and northern Baja California. *Science.* **219** (4590), 1287-1294 (1983).
3. Tachajapong, W., Lozano, J., Mahalingam, S., & Weise, D. R. Experimental modelling of crown fire initiation in open and closed shrubland systems. *Int. J. Wildl. Fire.* **23** (4), 451-462 (2014).
4. Rothermel, R. C., & Philpot, C. W. Predicting changes in chaparral flammability. *J. For.* **71** (10), 640-643 (1973).
5. Van Wagner, C. E. Conditions for the start and spread of crown fire. *Can. J. For. Res.* **7**, 23-34 (1977).
6. Fons, W. L. Analysis of Fire Spread in Light Forest Fuels. *J. Agric. Res.* (3) (1946).
7. Lozano, J. An investigation of surface and crown fire dynamics in shrub fuels. *Dissertation, University of California-Riverside.* 1-222 (2011).
8. Weise, D., Zhou, X., Sun, L., & Mahalingam, S. Fire spread in chaparral-'go or no-go?'. *Int. J. Wildl. Fire.* **14**, 99-106 (2005).
9. Cruz, M. G., Butler, B. W., Alexander, M. E., Forthofer, J. M., & Wakimoto, R. H. Predicting the ignition of crown fuels above a spreading surface fire. Part I: Model idealization. *Int. J. Wildl. Fire.* **15** (1), 47-60 (2006).
10. Cruz, M. G., Butler, B. W., Alexander, M. E., Forthofer, J. M., & Wakimoto, R. H. Predicting the ignition of crown fuels above a spreading surface fire. Part II: Model idealization. *Int. J. Wildl. Fire.* **15** (1), 47-60 (2006).

11. Li, J., Mahalingam, S., & Weise, D. R. Experimental investigation of fire propagation in single live shrubs. *Int. J. Wildl. Fire.* **26** (1), 58-70 (2017).
12. Byram, G. M. Combustian of Forest Fuels. *For. Fire Control Use.* 61-89 (1959).
13. Dupuy, J. L., Maréchal, J., & Morvan, D. Fires from a cylindrical forest fuel burner: Combustion dynamics and flame properties. *Combust. Flame.* **135** (1-2), 65-76 (2003).
14. Sun, L., Zhou, X., Mahalingam, S., & Weise, D. R. Comparison of burning characteristics of live and dead chaparral fuels. *Combust. Flame.* **144** (1-2), 349-359 (2006).
15. Fletcher, T. H., Pickett, B. M., *et al.* Effects of Moisture on Ignition Behavior of Moist California Chaparral and Utah Leaves. *Combust. Sci. Technol.* **179** (6), 1183-1203 (2007).
16. Engstrom, J. D., Butler, J. K., Smith, S. G., Baxter, L. L., Fletcher, T. H., & WEISE, D. R. Ignition Behavior of Live California Chaparral Leaves. *Combust. Sci. Technol.* **176** (9), 1577-1591 (2004).
17. Zukoski, E. Fluid Dynamic Aspects Of Room Fires. *Fire Saf. Sci.* **1**, 1-30 (1986).
18. Thomas, P. H., Webster, C. T., & Raftery, M. M. Some experiments on buoyant diffusion flames. *Combust. Flame.* **5**, 359-367 (1961).
19. Finney, M. a, Cohen, J. D., McAllister, S. S., & Jolly, W. M. On the need for a theory of wildland fire spread. *Intl J Wildl Fire.* **22** (1), 25-36 (2013).
20. Mendes-Lopes, J. M. C., Ventura, J. M. P., & Amaral, J. M. P. Flame characteristics, temperature-time curves, and rate of spread in fires propagating in a bed of Pinus pinaster needles. *Int. J. Wildl. Fire.* **12** (1), 67-84 (2003).
21. Williams, F. A. Mechanisms of fire spread. *Symp. Combust.* **16** (1), 1281-1294 (1977).
22. Sullivan, A. L., & Ball, R. Thermal decomposition and combustion chemistry of cellulosic biomass. *Atmospheric Environment.* **47**, 133-141 (2012).
23. Tachajapong, W., Lozano, J., Mahalingam, S., Zhou, X., & Weise, D. R. Experimental and Numerical Modeling of Shrub Crown Fire Initiation. *Combust. Sci. Technol.* 618-640 (2016).
24. Tachajapong, W., Lozano, J., Mahalingam, S., Zhou, X., & Weise, D. R. An investigation of crown fuel bulk density effects on the dynamics of crown fire initiation in Shrublands. *Combust. Sci. Technol.* **180** (4), 593-615 (2008).
25. Zhou, X., Weise, D., & Mahalingam, S. Experimental measurements and numerical modeling of marginal burning in live chaparral fuel beds. *Proc. Combust. Inst.* **30** (2), 2287-2294 (2005).
26. Pickett, B. M., Isackson, C., Wunder, R., Fletcher, T. H., Butler, B. W., & Weise, D. R. Flame interactions and burning characteristics of two live leaf samples. *Int. J. Wildl. Fire.* **18** (7), 865-874 (2009).
27. Cobian-Iñiguez, J., Sanpakit, C., *et al.* Laboratory Experiments to Study Surface to Crown Fire Transition in Chaparral. *Fall Meet. West. States Sect. Combust. Inst.* Paper #134HC-0040 (2015).
28. Silvani, X., & Morandini, F. Fire spread experiments in the field: Temperature and heat fluxes measurements. *Fire Safety J.* **44** (2), 279-285 (2009).
29. Morandini, F., Silvani, X., *et al.* Fire spread experiment across Mediterranean shrub: Influence of wind on flame front properties. *Fire Safety J.* **41** (3), 229-235 (2006).
30. Countryman, C. M., & Dean, W. A. Measuring moisture content in living chaparral: a field user's manual. *USDA For. Serv. Gen. Tech. Rep. PSW-36.* 28 <http://www.fs.fed.us/psw/publications/documents/psw_gtr036/> (1979).
31. Albini, F. A. A Model for Fire Spread in Wildland Fuels by- Radiation. *Combust. Flame.* **42** (July) (1985).
32. Rothermel, R. C. A Mathematical Model for Predicting Fire Spread in Wildland Fuels. *USDA For. Serv. Res. Pap. INT-115.* 40 (1972).
33. Freeborn, P. H., Wooster, M. J., *et al.* Relationships between energy release, fuel mass loss, and trace gas an aerosol emissions during laboratory biomass fires. *J. Geophys. Res. Atmos.* **113** (1), 1-17 (2008).
34. Finney, M. A., Cohen, J. D., *et al.* Role of buoyant flame dynamics in wildfire spread. *Proc Nat Acad Sci USA.* **112** (32), 9833-9838 (2015).
35. Green, L. R. Burning by prescription in chaparral. *USDA For. Serv. Gen. Tech. Rep. PSW-51.* 36 (1981).
36. Cohen, J., Bradshaw, B. Fire behavior modeling - a decision tool. *Proc. Prescr. Burn. Midwest State Art.* 1-5 (1986).
37. Weise, D. R., Koo, E., Zhou, X., Mahalingam, S., Morandini, F., & Balbi, J. H. Fire spread in chaparral - A comparison of laboratory data and model predictions in burning live fuels. *Int. J. Wildl. Fire.* **25** (9), 980-994 (2016).
38. Omodan, S. *Fire Behavior Modeling - Experiment on Surface Fire Transition to the Elevated Live Fuel A.* (March) (2015).
39. Mulvaney, J. J., Sullivan, A. L., Cary, G. J., & Bishop, G. R. Repeatability of free-burning fire experiments using heterogeneous forest fuel beds in a combustion wind tunnel. *Intl J Wildl Fire.* **25** (4), 445-455 (2016).

